Quantum phases and phase transitions of frustrated hard-core bosons on a triangular ladder

Tapan Mishra,[1] Ramesh V. Pai,[2] Subroto Mukerjee,[3,4] and Arun Paramekanti[5,6]
[1]*International Center for Theoretical Sciences, Bangalore 560 012, India*
[2]*Department of Physics, Goa University, Taleigao Plateau, Goa 403 206, India*
[3]*Department of Physics, Indian Institute of Science, Bangalore 560 012, India*
[4]*Centre for Quantum Information and Quantum Computing (CQIQC), Indian Institute of Science, Bangalore 560 012, India*
[5]*Department of Physics, University of Toronto, Toronto, Ontario, Canada M5S 1A7*
[6]*Canadian Institute for Advanced Research, Toronto, Ontario, Canada M5G 1Z8*
(Received 19 November 2012; published 9 May 2013)

Kinetically frustrated bosons at half filling in the presence of a competing nearest-neighbor repulsion support a wide supersolid regime on the two-dimensional triangular lattice. We study this model on a two-leg ladder using the finite-size density-matrix renormalization-group method, obtaining a phase diagram which contains three phases: a uniform superfluid (SF), an insulating charge density wave (CDW) crystal, and a bond ordered insulator (BO). We show that the transitions from SF to CDW and SF to BO are continuous in nature, with critical exponents varying continuously along the phase boundaries, while the transition from CDW to BO is found to be first order. The phase diagram is also found to contain an exactly solvable Majumdar Ghosh point, and reentrant SF to CDW phase transitions.

DOI: 10.1103/PhysRevB.87.174504 PACS number(s): 75.40.Gb, 67.85.−d, 71.27.+a

I. INTRODUCTION

Quantum phase transitions in low dimensional systems are of great interest because quantum fluctuations play a greater role in their physics than in their higher dimensional counterparts.[1,2] For instance in one-dimensional systems, quantum fluctuations can inhibit the appearance of long-range order that is seen in higher dimensional systems with the same symmetries. An example of this is the one-dimensional spin-1/2 Heisenberg chain with nearest-neighbor antiferromagnetic coupling which does not display any long-range Néel order unlike its two-dimensional square lattice counterpart. While quantum fluctuations in high dimensions maybe weak, geometrical frustration could prevent the occurrence of long-range order. A naive expectation might be that quantum fluctuations and geometrical frustration, when present together, would reinforce each other and severely inhibit ordering. However, there are several examples where the combination of frustration and quantum fluctuations induces interesting types of order such as through order-by-disorder transitions.[3] In one dimension, where quantum fluctuations are especially strong, their interplay with frustration can give rise to interesting phases and phase transitions such as the recently proposed chiral Mott insulator in frustrated Bose-Hubbard ladders, a phase with a gap to all excitations, and a staggered pattern of equilibrium currents.[4,5]

In this paper, we study a frustrated one-dimensional system of hard-core bosons. In this model a boson on a site can hop to a neighboring site (with amplitude t) and also feels a density-density interaction (of strength V) from occupied neighboring sites. In addition to these terms, there is also a frustrating next-nearest-neighbor hopping term (of amplitude t'). The Hamiltonian that describes this t-t'-V model is

$$H = -t\sum_i (a_i^\dagger a_{i+1} + \text{H.c.}) - t'\sum_i (a_i^\dagger a_{i+2} + \text{H.c.}) + \sum_i V n_i n_{i+1}, \quad (1)$$

where $a_i^\dagger$ and a_i are creation and annihilation operators for hard-core bosons at site i, and $n_i = a_i^\dagger a_i$ is the boson number operator at site i. Here we have the constraint that $a_i^{\dagger 2} = a_i^2 = 0$, which avoids multiple occupancies of the lattice sites. Frustration in this model arises from taking $t > 0$ and $t' < 0$. Further, $V > 0$ so that the interaction is repulsive. The model can be thought of as a zig-zag ladder of the sort shown in Fig. 1 with the nearest-neighbor and next-nearest-neighbor hopping arising from the motion of the bosons between and along the legs of the ladder, respectively. Note that this model does not have a simple representation in terms of spinless fermions due to the presence of the next-nearest-neighbor hopping term, which when expressed in terms of spinless fermions will not correspond to a simple hopping term. Thus, our model even with $V = 0$ is nontrivial and does not have a ground state corresponding to a filled Fermi sea. In fact, as we will see, for $V = 0$, aside from the trivial point $t' = 0$, there is only one other point corresponding to $t' = -t/2$, where the ground state can be obtained exactly.

Equation (1) can be mapped onto a spin-1/2 Hamiltonian by identifying $S_i^+ = a_i^\dagger$, $S_i^- = a_i$, and $S_i^z = (n_i - 1/2)$. Under this transformation the Hamiltonian (1) takes the form

$$H = \sum_i \big[-2t\big(S_i^x S_{i+1}^x + S_i^y S_{i+1}^y\big) + V S_i^z S_{i+1}^z - 2t'\big(S_i^x S_{i+2}^x + S_i^y S_{i+2}^y\big)\big]. \quad (2)$$

By making a spin rotation on one sublattice, to change the sign of the nearest-neighbor exchange coupling, Eq. (2) can be recast as an anisotropic (XXZ type) spin-$\frac{1}{2}$ model with a next-nearest-neighbor coupling. This model may then be viewed as a specific easy-plane deformation of the well-known SU(2) symmetric J_1-J_2 model which has been studied extensively.[6–9] The SU(2) symmetric J_1-J_2 model exhibits gapless to gapped transition at $J_2 \approx 0.241\,167$.[10] Interestingly, when $J_2 = J_1/2$, the quantum system dimerizes in the presence of frustration and is described by the Majumdar-Ghosh (MG) model.[11]

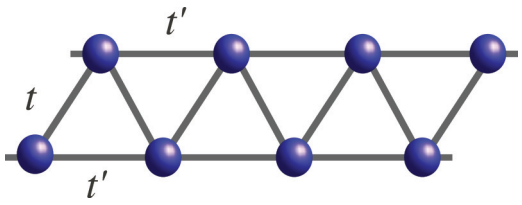

FIG. 1. (Color online) Zig-zag ladder system representing the t-t'-V model in one dimension. The arrows are the representation of the hopping directions. $t > 0$ and $t' < 0$.

Variants of the J_1-J_2 model with spin anisotropy have also been studied. The earliest such study was by Haldane who added an anisotropy parameter to the nearest-neighbor coupling term while the next-nearest-neighbor term was left isotropic.[12] More recently, a variant of the J_1-J_2 model with the same anisotropy in both the nearest-neighbor and next-nearest-neighbor terms has been studied.[13,14] Our model given by Eq. (2), while anisotropic in spin, is different from both the anisotropic models mentioned above in that it has only a single SU(2) symmetric point in parameter space (corresponding to $V = 2t$ and $t' = 0$) while the other two models have lines of points with SU(2) symmetry. Some of the salient features of our model like continuously varying critical exponents along the phase boundary and reentrant transitions are presumably due to the absence of such SU(2) symmetric lines, which will be discussed later. We will show that our model also has a point in parameter space analogous to the MG model when $V = 0$ and $t' = t/2$, but without SU(2) symmetry, where we can obtain the ground state exactly. The model at this point can be thought of as a U(1) analog of the MG model. Interest in this model also stems from the fact that the two-dimensional triangular lattice with such frustrated hard-core bosons has been shown to exhibit $\sqrt{3} \times \sqrt{3}$ supersolid phases.[15–17] Recently, a related model in one dimension with equal nearest- and next-nearest-neighbor hopping and nearest- and next-nearest-neighbor interactions has also been studied.[18]

In this paper, we study the model given by Eq. (1) at half filling numerically using the density matrix renormalization-group (DMRG) algorithm in the entire parameter space of $t' < 0$ and $V > 0$ with $t > 0$. We find that there are three phases, a superfluid (SF), bond-ordered (BO) phase and a charge density wave (CDW). These are analogs of the gapless spin liquid, gapped dimerized phase, and gapped Néel phase of the analogous anisotropic spin models. Our study mainly focusses on the phase boundaries and we show that the phase transitions in this model are of the Berezinski-Kosterlitz-Thouless (BKT) type and first order. Our results are shown in the phase diagram of Fig. 2. We find that along the lines of BKt transitions, there is a continuously varying critical exponent (corresponding to the Luttinger paramter). Another interesting feature of the phase diagram is a reentrant SF-CDW-SF transition that exists in a part of parameter space and whose origin can be understood in terms of an instability of the CDW state.

The remainder of the paper is organized as follows. In Sec. II, we study the MG point analytically and obtain the exact ground state to better understand the BO phase and in Sec. III, we study the CDW phase and obtain an analytical form for the phase boundary between this phase and the SF highlighting the reentrant phase transition. In Sec. IV, we describe the details of our DMRG study and give expressions for the various quantities that have been calculated and in Sec. V, we present our numerical results for the full phase diagram along with a discussion of its different features.

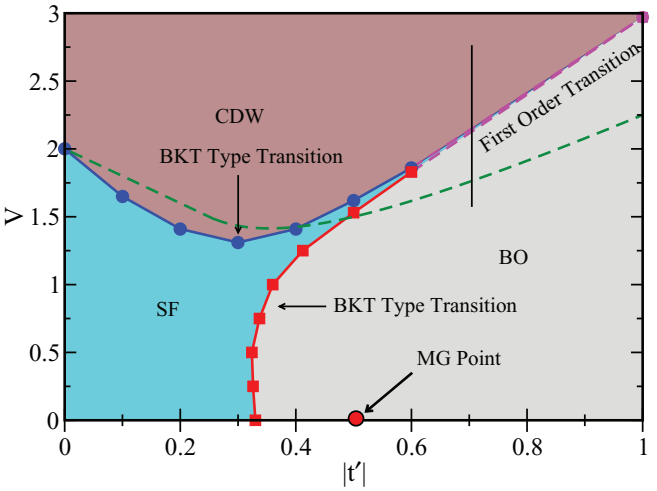

FIG. 2. (Color online) Phase diagram of the half filled t-t'-V model. There exist two gapless to gapped transitions, from SF to BO and SF to CDW for small $|t'|$ and V values, which are of the BKT type. There is also a direct transition from gapped BO to gapped CDW which is first order for large values of the interaction. The point at $|t'| = 0.5$ and $V = 0$ is the Majumdar-Ghosh point and the dashed line is the theoretically calculated instability line for the CDW state. The hopping amplitude is set to $t = 1$.

II. MAJUMDAR-GHOSH POINT

Consider the model $H = -\sum_i (t a_i^\dagger a_{i+1} + t' a_i^\dagger a_{i+2} + \text{H.c.})$ for hard-core bosons, where we have set the nearest-neighbor repulsion $V = 0$. We can rewrite this Hamiltonian in the language of spin-1/2 operators, which for $t' = -t/2$ is given by

$$H_{MG}^{xy} = \frac{t}{2} \sum_k \left[-3/2 + \sum_{\alpha=x,y} \left(S_k^\alpha - S_{k+1}^\alpha + S_{k+2}^\alpha \right)^2 \right].$$

Let us focus on a local state defined on three successive sites $(j, j+1, j+2)$, of the form $|\psi\rangle = |(\uparrow_j \downarrow_{j+1} + \downarrow_j \uparrow_{j+1}) \sigma_{j+2}\rangle$, where σ_{j+2} is an arbitrary spin state at site $j+2$. It is easy to show that

$$\left(S_j^x - S_{j+1}^x + S_{j+2}^x\right)|\psi\rangle = \tfrac{1}{2}|(\uparrow_j \downarrow_{j+1} + \downarrow_j \uparrow_{j+1})\bar{\sigma}_{j+2}\rangle, \quad (3)$$

where $\bar{\sigma}_{j+2}$ denotes the original spin at site $j+1$ being flipped. This means $(S_j^x - S_{j+1}^x + S_{j+2}^x)^2|\psi\rangle = \frac{1}{4}|\psi\rangle$. Similarly,

$$\left(S_j^y - S_{j+1}^y + S_{j+2}^y\right)|\psi\rangle = \frac{i\sigma_{j+2}}{2}|(\uparrow_j \downarrow_{j+1} + \downarrow_j \uparrow_{j+1})\bar{\sigma}_{j+2}\rangle, \quad (4)$$

so that $(S_j^y - S_{j+1}^y + S_{j+2}^y)^2|\psi\rangle = \frac{1}{4}|\psi\rangle$. Thus, the product state

$$\prod_{j \in even} |\uparrow_j \downarrow_{j+1} + \downarrow_j \uparrow_{j+1}\rangle \quad (5)$$

is an eigenstate of the Hamiltonian H_{MG}^{xy}, with energy per site $\frac{t}{2}(-3/2 + 1/2) = -t/2$. Since a sum of three spin-1/2

operators, such as $S^y_j - S^y_{j+1} + S^y_{j+2}$, cannot have a minimum eigenvalue of magnitude less than $1/2$, the state we have found is evidently a ground state. Another ground state, which is related by symmetry to the above ground state, is simply

$$\prod_{j\in odd} |\uparrow_j\downarrow_{j+1} + \downarrow_j\uparrow_{j+1}\rangle. \tag{6}$$

While we have not proved that these are the only two ground states of the Hamiltonian, our DMRG numerics indicate that this is the case. Note that the ground states obtained above are not products of singlets like the usual MG state and are thus not spin rotation invariant. This is not surprising since our Hamiltonian is also not spin rotation invariant unlike the J_1-J_2 model.

III. PHASE BOUNDARY OF THE CDW STATE AND THE SF-CDW-SF REENTRANT PHASE TRANSITION

Consider the CDW state, which in spin language may be denoted as $|\ldots\uparrow\downarrow\uparrow\downarrow\ldots\rangle$. Let us define Holstein-Primakoff bosons h, such that on the $\uparrow$ sites of the CDW, we have[19]

$$S^z_i = \left(\tfrac{1}{2} - h^\dagger_i h_i\right); S^+_i = h_i; S^-_i = h^\dagger_i, \tag{7}$$

while on the $\downarrow$ sites of the CDW, we have

$$S^z_i = \left(h^\dagger_i h_i - \tfrac{1}{2}\right); S^+_i = h^\dagger_i; S^-_i = h_i. \tag{8}$$

To quadratic order in the h bosons, we find that the Hamiltonian takes the form

$$H = -t\sum_i (h^\dagger_i h^\dagger_{i+1} + h_i h_{i+1}) + V\sum_i h^\dagger_i h_i - t'\sum_i (h^\dagger_i h_{i+2} + h^\dagger_{i+2} h_i). \tag{9}$$

Going to momentum space, and defining $\Psi^\dagger_k = (h^\dagger_k, h_{-k})$, we find the Hamiltonian

$$H = \sum_{k>0} \Psi^\dagger_k \begin{pmatrix} V - 2t'\cos 2k & -2t\cos k \\ -2t\cos k & V - 2t'\cos 2k \end{pmatrix} \Psi_k, \tag{10}$$

with eigenenergy $\lambda_k = \sqrt{(V - 2t'\cos 2k)^2 - (2t\cos k)^2}$. For large V, the spectrum has a gap $\sim V$. As V decreases, however, the spectrum develops a soft mode signaling an instability of the CDW state. For $|t'| < t/4$, the instability develops at $k = 0$ and $k = \pi$ below a critical repulsive interaction $V_{c,1} = 2(t - |t'|)$. For $|t'| > t/4$, the instability develops at *incommensurate* wave vectors, k_0 and $\pi - k_0$, where $k_0 = \cos^{-1}(\frac{t}{4|t'|})$, below a critical repulsive interaction $V_{c,2} = 2|t'| + \frac{t^2}{4|t'|}$. The instability line is thus nonmonotonic, with a minimum at $|t'| = \frac{1}{2\sqrt{2}}$, and it approximately follows the phase boundary of the CDW state found numerically using the DMRG. The nonmonotonicity of the instability line is responsible for the SF-CDW-SF reentrant phase transition as can be seen from Fig. 2.

IV. DMRG TREATMENT OF THE MODEL

We study the ground state of the model described by Eq. (1) using the finite-size DMRG method with open boundary conditions.[20,21] This method is best suited for (quasi-)one-dimensional problems.[21] For most of our calculations we study system sizes up to 300 sites and retain 128 density matrix eigenstates with the weight of the discarded states in the density matrix less than 10^{-6}. When $t' = 0$, the model can be solved exactly using the Bethe ansatz[22] and there exists a transition from a gapless SF to a gapped CDW phase like $(\ldots 10101010\ldots)$ phase at $V = 2t$. Here 1 (0) represents the presence (absence) of a boson at a particular site. However, as we will show when the value of t' is finite, the phase diagram is much richer. In the present work we calculate various different physical quantities to characterize the phases and phase transitions of our model. The resulting phase diagram is shown in Fig. 2.

We now list the various quantities we have calculated to identify the phases in our model. These quantities have been used previously to identify similar phases in related models.[23] In order to distinguish between the gapped and gapless phases we calculate the single-particle excitation gap,

$$G_L = E(L,N+1) + E(L,N-1) - 2E(L,N). \tag{11}$$

In Eq. (11), $E(L,N)$ is the ground-state energy of a system with L sites and N bosons.

The CDW phase and the transition into it can be studied by calculating the structure factor, which is the Fourier transform of the density-density correlation function,

$$S(k) = \frac{1}{L^2}\sum_{i,j} e^{ik(i-j)}(\langle n_i n_j\rangle - \langle n_i\rangle\langle n_j\rangle). \tag{12}$$

The BO phase has a nonzero value of the bond-order parameter,

$$O_{BO} = \frac{1}{L}\sum_i (-1)^i B_i, \tag{13}$$

where

$$B_i = \langle a^\dagger_i a_{i+1} + a^\dagger_{i+1} a_i\rangle, \tag{14}$$

and this is thus the quantity we calculate to identify this phase and the phase transition into it.

The commensurate-to-incommensurate transition can be tracked by identifying the k vector for ordering in a phase. This vector can be found by looking for a peak in the momentum distribution function,

$$n(k) = \frac{1}{L}\sum_{i,j} e^{ik(i-j)}\langle a^\dagger_i a_j\rangle. \tag{15}$$

Finally, to characterize the phase boundaries, we calculate the correlation function

$$\Gamma(r) = \langle a^\dagger_0 a_r\rangle, \tag{16}$$

which as we will see can be used to define the Luttinger parameter along the phase boundaries. In the remainder of the paper, we set $t = 1$.

V. RESULTS AND DISCUSSION

In the first part of this section we discuss the results of our calculation for $V = 0$. When $t' = 0$, the system is a gapless SF with finite momentum distribution at $k = 0$. As $|t'|$ increases, the system enters a gapped phase. The gapless-to-gapped transition can be seen by calculating the single-particle excitation gap as given in Eq. (11). We plot

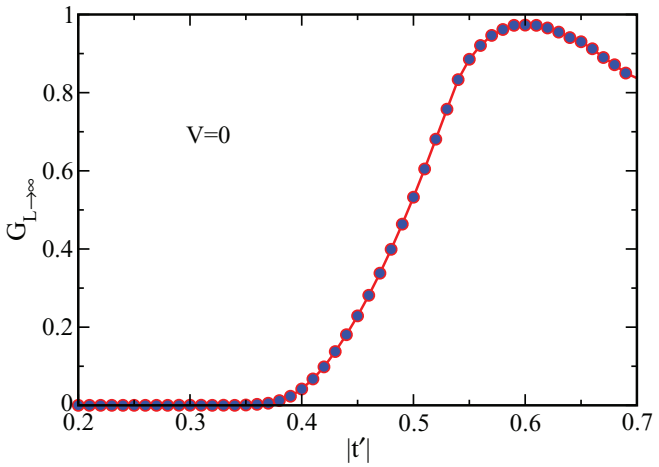

FIG. 3. (Color online) The extrapolated gap $G_L \to \infty$ plotted as a function of $|t'|$ for $V = 0$. The gapless to gapped phase transition occurs at $|t'| \approx 0.33$.

the extrapolated gap $G_{L\to\infty}$ as a function of $|t'|$ in Fig. 3. The extrapolation is done using a third-order polynomial in $1/L$. The transition point is located by observing where the extrapolated gap becomes of the order of 10^{-5}. In this way, we obtain the critical point for transition to the gapped phase at $|t'| \approx 0.33$. In Fig. 4 we show the polynomial extrapolation of the gap. It is clear that the gap slowly becomes nonzero for values of $|t'| > 0.33$. While this extrapolation method works for the gap in our system, there could in general be subtleties related to extrapolation of the gap and other quantities obtained from calculations on finite-sized systems to the thermodynamic limit.[24]

The gap arises because of frustration which tries to make the ground state have a bond order (BO) of the sort described in our analysis of the MG point. The bond energy is different for odd and even bonds in this phase. This emergence of the BO phase can be tracked by calculating the BO order parameter (O_{BO}) as given in Eq. (13). In the BO phase, O_{BO} is finite in the thermodynamic limit and vanishes for small values of $|t'|$. We plot O_{BO} as a function of $|t'|$ in Fig. 5

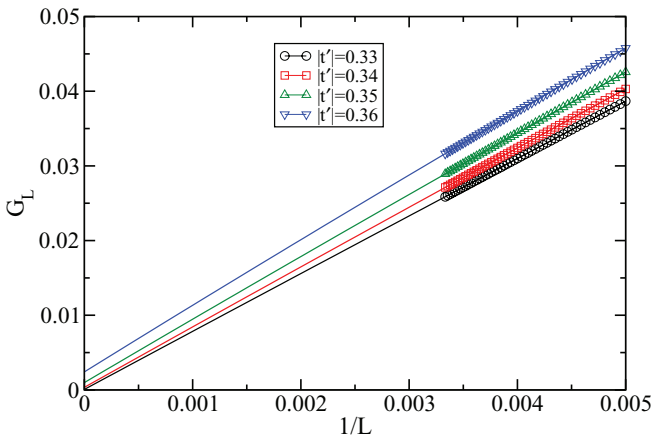

FIG. 4. (Color online) Polynomial fitting of the gap shows that the gap slowly goes to zero for $|t'| \approx 0.33$. The symbols are the numerical data and the lines are the fits.

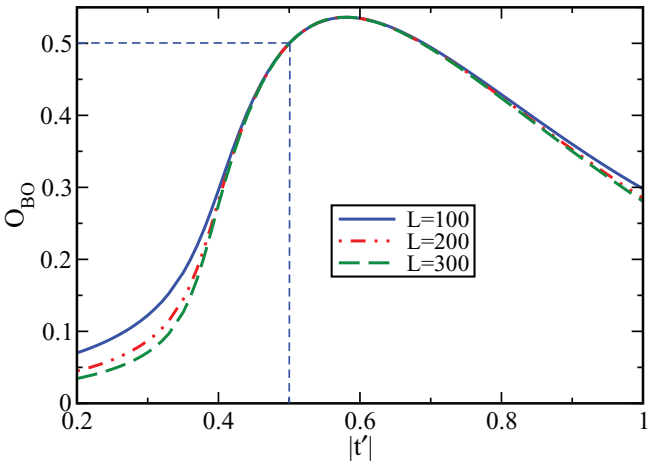

FIG. 5. (Color online) O_{BO} is plotted as a function of $|t'|$ for $L = 100$, 200, and 300. The increases of the value of O_{BO} as $|t'|$ increases indicates the transition to the BO phase. The vertical dashed line indicates the location of the MG point and the horizontal dashed line is the value of O_{BO} at this point, which is 0.5 independent of system size.

for three different lengths, $L = 100$, 200, and 300. The value of O_{BO} is maximum at $|t'| \approx 5.9$ and decreases on either side of the maximum. To the left of the maximum, i.e., when $|t'|$ decreases, the jump becomes sharper and sharper as the length increases and appears to be saturating to a small value as $|t'|$ decreases. At $|t'| = 0.5$ the value of $O_{BO} = 0.5$ and independent of length as expected for the MG point.

Our analysis of Sec. III shows that there is a commensurate-to-incommensurate transition at $|t'| = 0.25$. We can verify this by calculating the momentum distribution $n(k)$ as a function of k as shown in Fig. 6. Here we see that the momentum distribution has one maximum at $k = 0$ up to about $|t'| \approx 0.5$ after which the maxima shift to values of $k \neq 0$. This indicates the commensurate-to-incommensurate transition. The peak position shifts towards $k = \pm\pi/2$ as $|t'| \to \infty$ where the

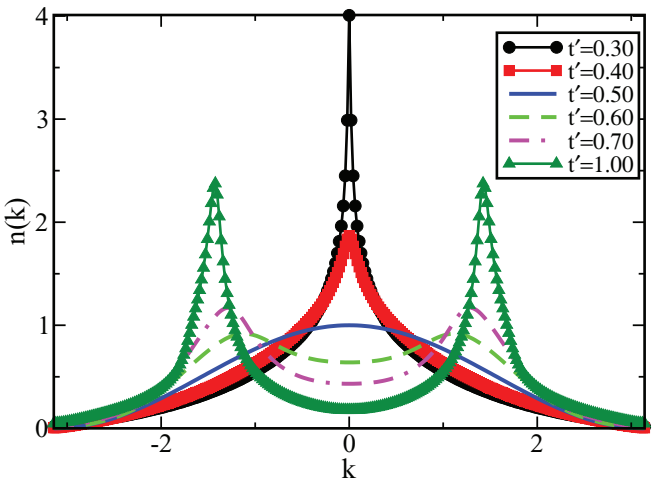

FIG. 6. (Color online) Momentum distribution $n(k)$ is plotted for different $|t'|$. There exists a commensurate-to-incommensurate transition at $|t'| > 0.5$ which can be seen as the onset of two peaks at $k \neq 0, \pi$.

two-leg ladder can be considered as a single chain. The fact that the transition does not occur at $|t'| = 0.25$ can be attributed to the hard-core nature of the bosons. The analysis of Sec. III assumed noninteracting particles.

Now we turn our attention to $V \neq 0$. When $|t'| = 0$ it is known that at $V = 2$, the model exhibits a transition from SF to the CDW phase.[22] As the value of $|t'|$ is increased we get three different scenarios:

(1) SF-CDW transition as a function of V for small values of $|t'|$.

(2) BO-SF-CDW as a function of V for intermediate values of V.

(3) BO-CDW transition as a function of V for large values of $|t'|$.

It is to be noted that the SF phase is gapless where as the BO and CDW phases are gapped. When the value of $|t'|$ is small, the SF-CDW transition occurs at $V < 2$ since the presence of negative $|t'|$ suppresses the effect of t. This allows the bosons to stabilize in the CDW ground state even for a small nearest-neighbor interaction. This can be seen from Fig. 2 where the upper phase boundary represents the SF-CDW transition for small values of $|t'|$. As $|t'|$ increases the value of V at which the transition takes place decreases gradually until it reaches a minimum and then increases again as expected from the analysis of Sec. III. This indicates a reentrant phase transition where at fixed V, an increase of $|t'|$ will drive the system from SF to CDW and back to SF again. It is interesting to note that the lowest point of the phase boundary obtained from the numerics is not too far from that predicted from the analytical calculation of Sec. III.

The phase boundary between the SF and BO phases is also shown in Fig. 2. This boundary originates at $V = 0$ and $|t'| = 0.33$ and moves upwards as shown. The superfluid region is pinched off by the approach of the SF-BO phase boundary towards the SF-CDW boundary. Crudely speaking, V prefers the formation of CDW order, $|t'|$ favors BO, while the nearest-neighbor hopping causes SF order. As long as both V and $|t'|$ are smaller than or close to 1, the nearest-neighbor hopping term ensures that the transition from BO to CDW has an intervening region of SF. However, once V and $|t'|$ start becoming larger than 1, there is a direct transition from CDW to BO, which appears to be first order from our calculations.

We now discuss our characterization of these transitions. It is known that for $t' = 0$, the transition from SF-CDW exhibits a BKT-type scaling of the gap. The correlation function $\Gamma(r) \sim 1/r^{\eta}$ with $\eta = 1$ at the critical point with an antiferromagnetic modulation and also a log correction. We find a similar BKT-type scaling of the gap along both the SF-CDW phase boundaries and SF-BO phase boundaries. The scaling of the gap at the BKT transition can be used to locate the critical point of the transition fairly accurately.[23] The critical exponent η can also be measured along the phase boundaries and we find this exponent to be varying continuously along both phase boundaries. We do not have the numerical accuracy to track this variation all the way up to the point where the boundaries appear to merge. It appears that there is a first phase transition from BO to CDW for larger values of $|t'|$ and V. In the following subsections, we present data supporting each of these claims.

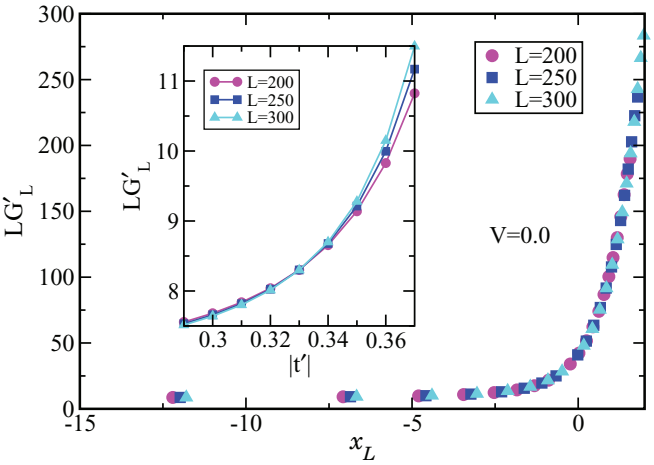

FIG. 7. (Color online) The scaled gap LG'_L is plotted as a function of x_L. Inset: The scaled gap plotted as a function of $|t'|$ for $V = 0$. This shows the SF-to-BO transition at $|t'| = 0.33$.

A. BKT scaling and gapless-to-gapped transition

Since the SF phase is gapless and the BO and CDW phases are gapped, we can use scaling of the gap G_L given by Eq. (11) to locate the transition. G_L is computed for lattices up to 300 sites. At the BKT transition from SF to BO the gap closes as

$$G \sim \exp\left[-\frac{a}{\sqrt{||t'| - |t'_c||}}\right], \tag{17}$$

where a is a constant.

The correlation length ξ, which scales at the critical point as the inverse of the gap, is finite in the gapped phase and diverges in the gapless SF phase. We use the following finite-size-scaling relation for the gap in the region close to the phase transition,

$$LG_L \times \left(1 + \frac{1}{2\ln L + C}\right) = F\left(\frac{\xi}{L}\right), \tag{18}$$

where F is a scaling function and C is an unknown constant to be determined (see Fig. 7). In the region close to the critical point and within the SF phase, the values of $F(\xi/L)$ is expected to be system-size independent, i.e., plots of $LG'_L = LG_L[1 + 1/(2\ln L + C)]$ as a function of t' for different system sizes should intersect in that region. Also, the curves obtained by plotting LG'_L as a function of ξ/L for several values of L should be system-size independent. Therefore, the plots of LG'_L as a function of $x_L = \ln L - \ln \xi$ for different lengths collapse in the critical region. We obtain the values of a, C, and $|t'_c|$ for the best possible collapse of the data in the gapped side where the correlation length diverges as $\xi \sim \exp[a/\sqrt{||t'| - |t'_c||}]$. A similar procedure can be used for the other part of the phase diagram, i.e., the SF-to-CDW transition by replacing $|t'|$ by V. The accuracy of this method has been tested by locating the Heisenberg point at $t' = 0$.[23] It is found to be at $V = 2.02 \pm 0.01$, very close to the analytical result. Here, we also find the critical point for the SF-to-BO transition at $|t'| = 0.33 \pm 0.01$ for $V = 0$ which is consistent with the value obtained previously in equivalent spin models.[25]

We use the above technique to obtain the boundaries between gapped and gapless phases in the phase diagram

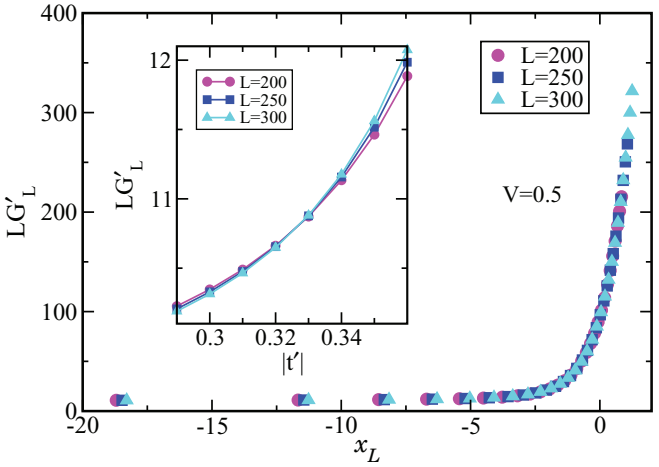

FIG. 8. (Color online) The scaled gap LG'_L is plotted as a function of x_L. Inset: The scaled gap plotted as a function of $|t'|$. This shows the SF-to-BO transition at $|t'| = 0.32$.

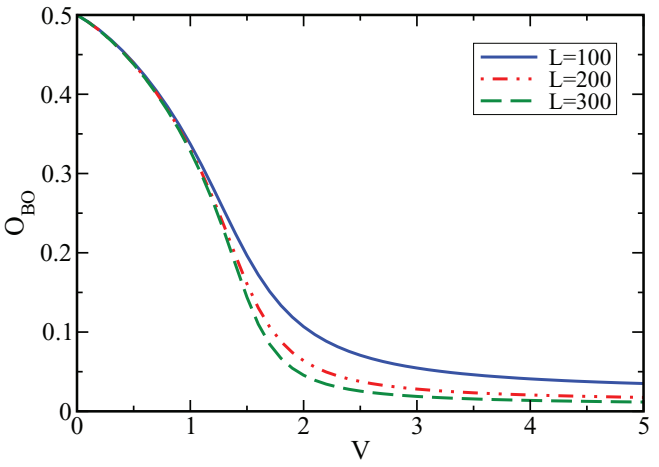

FIG. 10. (Color online) O_{BO} is plotted as a function of V at $|t'| = 0.5$ for different lengths.

Fig. 2. Another possible way to obtain the boundary is to extrapolate the gap to $L \to \infty$ and locate the points at which it goes from being nonzero to zero. However, we find that the former technique is more accurate than the latter one and thus we use the BKT scaling form of the gap to locate the transition. In Fig. 8 we show the scaling of the gap along the SF-BO transition boundary. The collapse of the curves is obtained by plotting LG'_L vs x_L within the gapped phase for $|t'_c| = 0.325 \pm 0.005$ and $V = 0.5$(main panel). The plots of LG'_L vs $|t'|$ (insets), for $V = 0.5$ and for three values of L show that the LG'_L curves intersect at the critical point $|t'| = 0.32$. Similarly in Fig. 9, we show the collapse of the LG'_L vs x_L data for $|t'| = 0.3$ when $V = 1.31$ (main panel) and the intersection of the LG'_L vs V curves for different lengths at the critical point (inset).

We now verify the locations of the SF-BO and SF-CDW phase boundaries by using the scaling of the BO order parameter and the density-density structure factor. In the BO phase O_{BO} is finite and zero in the SF phase. The value of O_{BO} is equal to 0.5 at the MG point. In order to see the the transition from BO to SF and then to CDW we start from the MG point, i.e., from $|t'| = 0.5$, and then move along the V axis. In Fig. 10 we plot O_{BO} as a function of V for $L = 100, 200, 300$. It can be seen that the value of O_{BO} decreases as we increase V. The decrease is faster for large lengths decrease implying that O_{BO} tends to zero in the thermodynamic limit. In order to see the actual transition point we perform a finite-size scaling of O_{BO}.[23,26] In Fig. 11, we plot O_{BO} as a function of $L^{-0.5}$ for different values of V and then extrapolate to $L \to \infty$. It is evident that the curve for $V = 1.6$ extrapolates to zero and the curves for $V > 1.6$ extrapolate to finite values showing the transition to the BO phase for values of $V \approx 1.5$. This result is in accordance with the phase diagram obtained by scaling of the gap where the transition point for the BO-to-SF transition is at $V = 1.53$. In order to understand the SF-CDW transition we perform a similar scaling of the density-density structure factor as given in Eq. (12) (see Fig. 12). An extrapolation shows that the $S(\pi)$ for $V \geqslant 1.6$ tends to a finite value in the thermodynamic limit. However, for values of $V < 1.6$ the curves appear to extrapolate to zero. This is also in accordance

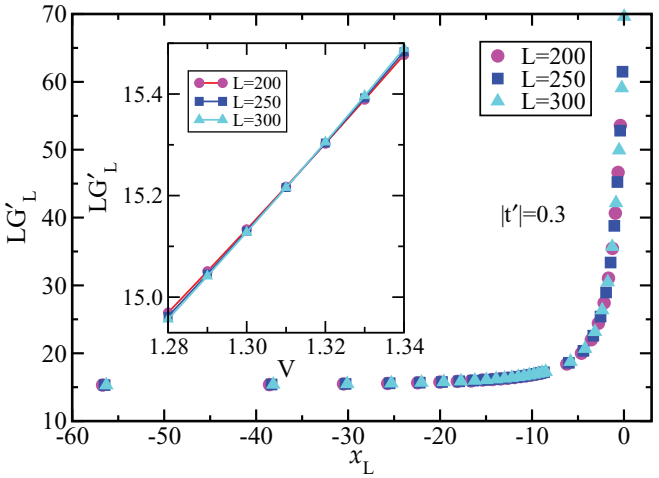

FIG. 9. (Color online) The scaled gap LG'_L is plotted as a function of x_L. Inset: The scaled gap plotted as a function of V. This shows the SF-to-CDW transition at $V = 1.31$.

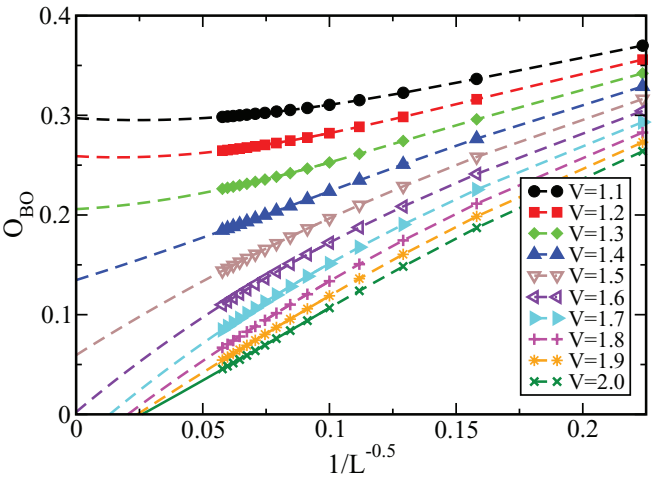

FIG. 11. (Color online) O_{BO} is plotted as a function of $1/L^{-0.5}$ for different V at $|t'| = 0.5$ showing the BO-SF transition.

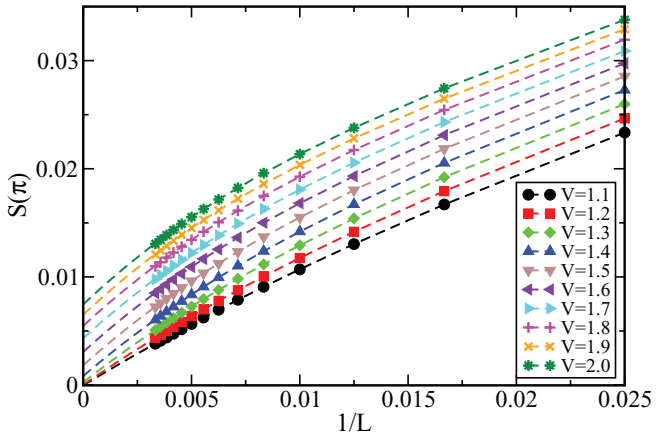

FIG. 12. (Color online) Finite-size scaling of $S(\pi)$ shows the SF-CDW transition.

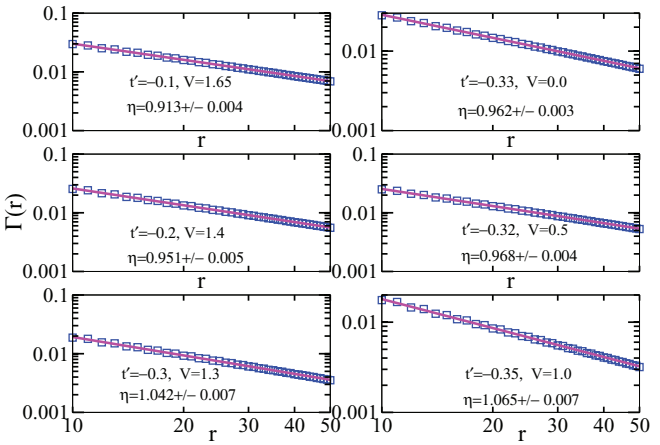

FIG. 13. (Color online) $\Gamma(r)$ plotted as a function of r for $10 \leqslant r \leqslant 50$. The left panel is for the critical points along the SF-CDW boundary and the right panel is along the SF-BO boundary of the phase diagram shown in Fig. 2. The symbols are the value of $\Gamma(r)$ and the solid lines are the fitted function of the form a/r^{η}. The errors are obtained from the linear fit to the data. It can be clearly seen that the value of η increases by increasing the values of V and $|t'|$ as we move along the SF-CDW and SF-BO, respectively.

with the phase diagram where the SF-CDW transition occurs at $V = 1.62$ for $|t'| = 0.5$

B. Critical exponent across the phase boundary

We now compute the critical exponents across the two BKT phase boundaries representing the SF-CDW and SF-BO transition. This exponent η is defined by the relation

$$\Gamma(r) \sim 1/r^{\eta}, \tag{19}$$

where $r = |i - j|$, and i and j are the lattice indices. η can thus be obtained by means of a straight-line fit to $\Gamma(r)$ as a function of r on a log-log scale. To avoid boundary effects, which can corrupt such a fit, we discard data obtained from the edges of our numerical system and use only data obtained from the bulk. The exponent η obtained this way will have a dependence on system size and the number of DMRG states kept in the calculation, which we have investigated. The plots of $\Gamma(r)$ vs r are shown in Fig. 13 for different points along the phase boundaries for $L = 500$ and 128 states. About 50 sites from the bulk were used for the fit. The error bars mentioned are for the linear fits to the data. The values of η, while always close to 1, seem to be varying along parts of the phase boundaries. η was found to decrease for all points with increasing L and increasing number of DMRG states, so it is reasonable to believe that $\eta < 1$ along sections of the phase boundary. We find $\eta > 1$ for some parts of the phase boundary such as $t' = -0.3, V = 1.3$ and $t' = -0.35, V = 1.0$ and it is likely that the value of η for these points will eventually go to 1 or lower with increasing system size and number of DMRG states which will have to be confirmed by more extensive numerical calculations. Further, the error in η introduced due to the error in the determination of the critical points is minuscule and less than that due to the linear fits.

As can be seen from Fig. 13, η appears to be increasing as we move to larger values of $|t'|$ along the SF-CDW boundary. It is known that $\eta = 1$ exactly at $t' = 0$ but from our data it appears that η drops as soon as a nonzero t' is introduced and once again rises towards 1. Along the other phase boundary, η starts from a value close to but less than 1 and increases as we move along it to larger values of V. It is likely that the two boundaries merge exactly at the point where $\eta = 1$, which is also where the line of first-order transitions begins (a multicritical point). Another possibility is that the two phase boundaries merge before the line of first-order points begins and there is an intermediate section along the phase boundary between CDW and BO, where η varies continuously, i.e., the transition is Gaussian in nature. At the moment, we do not have the numerical accuracy to resolve these two scenarios.

It is interesting to note that we obtain a value of η different from 1 and changing continuously at least along parts of the boundaries. This is not the case for previously studied anisotropic spin models. It has been argued that in those models, the value of η is pinned to 1 along both the SF-CDW and SF-BO phase boundaries.[12–14] A renormalization-group (RG) analysis of the sine-Gordon theory for these models shows that this is due to the fact that the zero umklapp line intersects a line of SU(2) invariant points in the phase space of the models.[12] The point of intersection happens to be the transition point from spin fluid (SF in the language of hard-core bosons) to dimer order (BO in the language of hard-core bosons) and has $\eta = 1$. The RG flow along both phase boundaries is towards this point thus pinning the exponent along them to 1. Further, in this RG analysis, the transition from CDW to BO is always continuous with a continuously varying $\eta > 1$, a Gaussian transition.

Our model does not have an SU(2) symmetric point separating the SF and BO phases or a line of SU(2) symmetric points in parameter space and thus will not have the same RG flow diagram. There is hence no reason *a priori* to expect the η value to be pinned to 1 along the phase boundaries. However, since the transition out of the SF phase might still be expected to be governed by a sine-Gordon theory in which umklapp is not relevant, η should be less than or equal to 1 along these boundaries. Thus, it can be expected that the values of $\eta > 1$ we seem to obtain for certain points along the phase boundaries

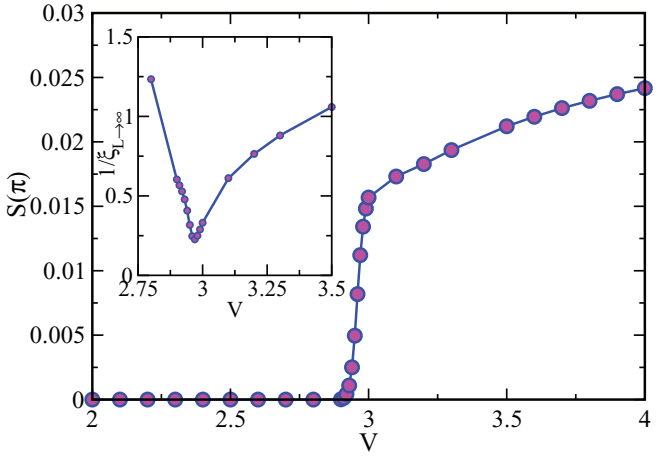

FIG. 14. (Color online) $S(\pi)$ is plotted as a function of V for $|t'| = 1.0$ showing the BO-CDW transition. Inset: The $1/\xi_{L\to\infty}$ is plotted as a function of V to confirm the first-order nature of the BO-CDW transition.

will settle down to 1 or lower as the system size and number of DMRG states are increased.

An analytical understanding of the phase boundaries and critical exponents will require a detailed field-theoretical study of the underlying sine-Gordon-type action, which will be presented in a separate paper.

C. Gapped-to-gapped phase transition

In this section we study the transition from the BO to the CDW phase at large $|t'|$ values. For $|t'| > 0.6$ the SF phase shrinks very slowly and appears to finally disappear at $|t'| \approx 0.7$. After this point the BO phase slowly undergoes a direct transition to the CDW phase. To study the phase transition we use the CDW structure factor as an order parameter. We plot the extrapolated values of $S(\pi)$ as a function of V in Fig. 14 for $|t'| = 1.0$. The sudden jump in the value of $S(\pi)$ at $V \approx 2.9$ implies a first-order transition from the BO to the CDW phase. This transition is further verified by examining the correlation

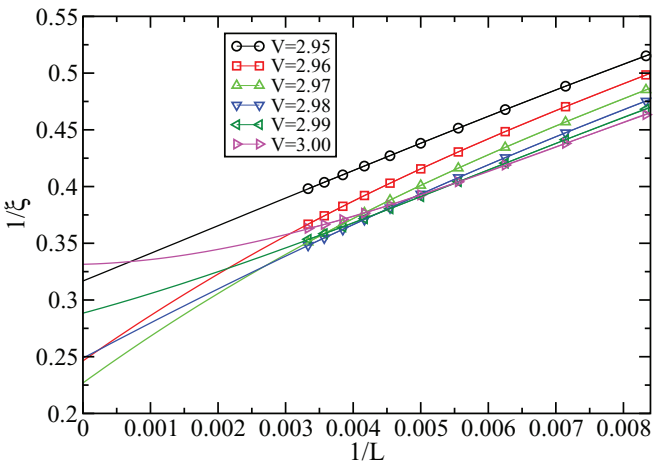

FIG. 15. (Color online) Numerical data for $1/\xi_{L\to\infty}$ vs $1/L$ (symbols) and fits (lines) plotted for different values of V to confirm the first-order nature of the BO-CDW transition.

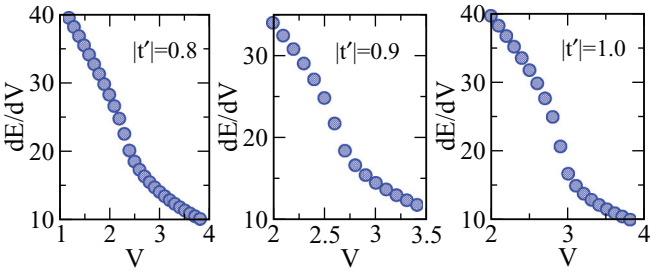

FIG. 16. (Color online) The derivative of the ground-state energy with respect to V as a function of V. A discontinuity appears in the first derivative, showing that the ground-state energy has a kink as a function of V, indicating a discontinuous transition. The "latent heat," proportional to the magnitude of the discontinuity, seems to increase with increasing $|t'|$.

length of the system. At the first-order transition the single-particle excitation gap remains finite. As mentioned earlier, the correlation length $\xi \propto 1/G$. Therefore at the first-order transition $1/\xi$ should remain finite. We show the extrapolated values of $1/\xi_{L\to\infty}$ in the inset of Fig. 14. It is evident from the figure that while approaching the transition from the BO side, $1/\xi_{L\to\infty}(G_L)$ decreases rapidly, reaches a minimum at the transition point $V = 2.97$, and then increases as the system enters the CDW phase. The extrapolation is done using a third-order polynomial in $1/L$ and is shown in Fig. 15. The gap remains finite at the minimum implying the absence of an SF phase. A further indicator of the first-order nature of the transition comes from looking at the derivative of the ground-state energy with respect to V, dE/dV, shown in Fig. 16 for different values of $|t'|$. It can be seen that there is the appearance at a discontinuity in the derivative, which seems to get more pronounced with $|t'|$. This shows that the transition is discontinuous and the "latent heat" associated with it increases as one moves up the phase boundary.

The sine-Gordon theory for the CDW-to-BO transition predicts a continuous transition with $\eta > 1$ varying continuously along the phase boundary.[12] However, it has been pointed out that this analysis ignores higher-order umklapp terms, which can drive the transition first order, which is what we appear to be seeing here.[13] We emphasize, once again, that we do not have the resolution to clearly say if the first-order line begins from the point of intersection of the SF-CDW and SF-BO phase boundaries. There could be a small section of the phase boundary where the Gaussian transition between CDW and BO is seen. However, our numerics suggest that for sufficiently large values of V along the CDW-BO phase boundary, the transition is of first order. We note that phase diagrams of the sort we have found can also be obtained from entanglement based studies of microscopic models such as in spin models on frustrated ladders[27] and the extended Hubbard model.[28] Problems relating to finite-size effects in calculations of the entanglement are also discussed in the above references.

VI. CONCLUSION

We have presented a detailed study of the hard-core boson in a one-dimensional lattice in the presence of frustrated

next-nearest-neighbor hopping and the nearest-neighbor interaction using the finite-size DMRG method. The ground-state phase diagram has three phases, SF, CDW, and BO, with continuous transitions along the SF-CDW and SF-BO phase boundaries and first-order transitions along the CDW-BO phase boundary. The SF-CDW phase boundary is not monotonic giving rise to a reentrant phase transition. Further, from numerical data for our system sizes and density-matrix states, the critical exponent η appears to be different from 1 varying continuously along the SF-CDW and SF-BO phase boundaries in contrast to other anisotropic frustrated models.

ACKNOWLEDGMENTS

S.M. thanks the Department of Science and Technology (DST) of the government of India for support. R.V.P. thanks University Grants Commission (UGC) of the government of India for support. A.P. was funded by NSERC of Canada, and acknowledges support from the International Center for Theoretical Sciences (Bangalore) during the initial stages of this project. The authors would like to thank D. Sen, T. Giamarchi, and L. Santos for very useful discussions.

[1] S. Sachdev, *Quantum Phase Transitions* (Cambridge University Press, Cambridge, England, 2002).

[2] T. Giamarchi, *Quantum Physics in One Dimension* (Oxford University Press, Oxford, 2004).

[3] G. Misguich and C. Lhuillier, *Frustrated Spin Systems*, edited by H. T. Diep (World Scientific, Singapore, 2004).

[4] A. Dhar, M. Maji, T. Mishra, R. V. Pai, S. Mukerjee, and A. Paramekanti, Phys. Rev. A **85**, 041602 (2012).

[5] A. Dhar, T. Mishra, M. Maji, R. V. Pai, S. Mukerjee, and A. Paramekanti, Phys. Rev. B **87**, 174501 (2013).

[6] T. Tonegawa, and I. Harada, J. Phys. Soc. Jpn. **56**, 2153 (1987).

[7] R. J. Burshil G. A. Gehring, D. J. J. Farnell, J. B. Parkinson, C. Zeng, and T Xiang, J. Phys.: Condens. Matter **7**, 8605 (1995).

[8] R. Chitra, S. Pati, H. R. Krishnamurthy, D. Sen, and S. Ramasesha, Phys. Rev. B **52**, 6581 (1995).

[9] S. R. White, and I. Affleck, Phys. Rev. B **54**, 9862 (1996).

[10] S. Eggert, Phys. Rev. B **54**, R9612 (1996).

[11] C. K. Majumdar, and D. K. Ghosh, J. Math. Phys. **10**, 1388 (1969).

[12] F. D. M. Haldane, Phys. Rev. B **25**, 4925 (1982).

[13] S. Furukawa, M. Sato, and A. Furusaki, Phys. Rev. B **81**, 094430 (2010).

[14] S. Furukawa, M. Sato, S. Onoda, and A. Furusaki, Phys. Rev. B **86**, 094417 (2012).

[15] H. C. Jiang, M. Q. Weng, Z. Y. Weng, D. N. Sheng, and L. Balents, Phys. Rev. B **79**, 020409(R) (2009).

[16] V. G. Rousseau and P. J. H. Denteneer, Phys. Rev. Lett. **102**, 015301 (2009).

[17] S. D. Bennett, L. Cockins, Y. Miyahara, P. Grütter, and A. A. Clerk, Phys. Rev. Lett. **104**, 017203 (2010).

[18] D. Rossini, V. Lante, A. Parola, and F. Becca, Phys. Rev. B **83**, 155106 (2011).

[19] T. Holstein and H. Primakoff, Phys. Rev. **58**, 1098 (1940).

[20] S. R. White, Phys. Rev. Lett. **69**, 2863 (1992).

[21] U. Schollwöck, Rev. Mod. Phys. **77**, 259 (2005).

[22] M. A. Cazalilla, R. Citro, T. Giamarchi, E. Orignac, and M. Rigol, Rev. Mod. Phys. **83**, 1405 (2011).

[23] T. Mishra, J. Carrasquilla, and M. Rigol, Phys. Rev. B **84**, 115135 (2011).

[24] G. Barcza, Ö. Legeza, R. M. Noack, and J. Sólyom, Phys. Rev. B **86**, 075133 (2012).

[25] K. Nomura, and K. Okamoto, J. Phys. A: Math. Theor. **27**, 5773 (1994).

[26] S. Ejima and S. Nishimoto, Phys. Rev. Lett. **99**, 216403 (2007).

[27] E. H. Kim, Ö. Legeza, and J. Sólyom, Phys. Rev. B **77**, 205121 (2008).

[28] C. Mund, Ö. Legeza, and R. M. Noack, Phys. Rev. B **79**, 245130 (2009).